POLITECNICO
MILANO 1863

SCUOLA DI INGEGNERIA INDUSTRIALE
E DELL'INFORMAZIONE

Executive Summary of the Thesis

Enhancing Gas Turbine Simulation for Hydrogen-Powered Aircraft

Laurea Magistrale in Energy Engineering - Ingegneria Energetica

Author: Riccardo Di Loreto

Advisor: Prof. Paolo Chiesa

Academic year: 2022-2023

1. Introduction

Civil aviation, a linchpin in the global transportation network fostering economic growth, faces a pressing need for next-generation aircraft to markedly reduce climate impacts. In 2022, international passenger activity doubled, nearing pre-Covid levels, signaling a potential growth resurgence from early 2023 [1]. The aviation sector's contribution to global CO_2 emissions reached 2%, outpacing other transport modes in 2022 [1].

This study primarily delves into the operational aspects of transitioning from conventional jet fuel to hydrogen for aircraft engines.

Hydrogen-powered aircraft offer emission-free flight potential but grapple with technical and economic challenges. Low volumetric energy density poses design challenges for aircraft accommodating larger fuel volumes. Liquefied hydrogen emerges as a favored storage option in this regard, despite challenges in handling and storage.

This thesis work stems from the participation of the Department of Energy of the Politecnico di Milano in a European project called EFACA (Environmentally Friendly Aviation for All Classes of Aircraft). The EFACA project focuses on six main objectives:

1. design, develop, and test a novel hybrid propulsion system combining a gas turbine engine with an electric motor;
2. conduct comparative tests on two hydrogen fuel cell configurations;
3. test a complete liquid hydrogen power system, from the cryogenic tank to fuel vaporization and combustion;
4. design an 80-seat turboprop aircraft with a 1000 km range using hybrid turboelectric propulsion;
5. design a 150-seat jetliner with a 2000 km range utilizing liquid hydrogen fuel.

This thesis aligns with objective n°3, undertaking a comprehensive numerical analysis of the system using proprietary software developed by Politecnico di Milano.

After providing an overview of the relevant studies in the aeronautical sector (Section 2), the methodology for calculating the cycle will be defined (Section 3). Components "air intake" and "nozzle" had to be added to the existing routines, their mathematical model will be outlined in Section 3. Section 4 details the reference engine chosen for model validation and discusses changes to the cycle architecture to exploit the potential of liquid hydrogen. Section 5 presents the results obtained, explaining their effects and implications. The final conclusions and proposed ideas for future developments are reported in Section 6.

2. Literature review

The definition of the optimal design of the aircraft engine starts from the selection of the type of propulsion system to be adopted. This decision should consider both design constraints and environmental factors. Then, based on the engine foundational architecture, potential enhancements will be evaluated. Fuel cells appear to be the dominant choice for small, short-range aircraft, while hydrogen combustion dominates for large, long-range aircraft [6]. This is because combustion engines have higher specific power and fewer thermal management challenges.
Most of today's commercial aircraft are powered by the fuel-efficient turbofan engines. This work will focus on this type of engine.
The concept of a hydrogen-powered gas turbine remains the same as kerosene-powered engines. Because of the high specific power and historical engineering experience with turbomachinery, hydrogen combustion is the proposed solution for many hydrogen aircraft, particularly those from airframers and aircraft engine manufacturers [2] [3].
Studies on thermodynamic analyses of alternative-fueled aviation engines are relatively limited compared to those on conventional fuel utilization. Some of the most relevant for this work are reported below.
In 2000, the European Commission funded the Cryoplane study [17]. Different aircraft configurations were studied where engine design were unaltered when converting from kerosene to hydrogen. The study concluded that, due to the excessive tank volume required for LH_2, energy consumption would increase by 9-14%.
To estimate the potential of using LH_2 in a turbofan engine, Lockheed-California Company conducted a study for NASA-Langley Research Center in 1976-1978 [7]. Two concepts for improved performance were evaluated in this study: compressor air intercooling and cooling of turbine coolant flow with LH_2 allow respectively a 1.86% and a 0.53% improvement in fuel consumption thanks to decreased compressor work and coolant flow rate reduction.
Although previous research has explored the thermodynamic potential of liquid hydrogen as a turbofan engine fuel, this study leverages in-house software equipped with advanced cooled-turbine calculation routines [8].

3. Calculation methodology

In this section, it will be described the program used for engine simulation and the integration of missing air intake and nozzle components into it.

3.1. The GS code: background informations and working principles

This study utilizes the in-house software "Gas Steam" (GS) for performance predictions, developed at Politecnico di Milano's Energy Department since the early 90s. Programmed in Fortran 90, GS offers accurate results for various power and chemical plant configurations. The software, explained in detail by Chiesa and Macchi [8], assembles modules to replicate plant configurations, allowing parameter adjustments for components. The iterative computational nature of GS requires an initial approximation. This initial solution consists of pressure, mass flow, temperature, and composition data for all the thermodynamic points within the system. During a calculation run, mass and energy balances are computed sequentially for each component, applying appropriate operating characteristics and constraints. The iterative process continues until convergence is achieved. Thanks to its modular nature, GS enables the integration of new components like nozzles and air intakes, typical of aircraft applications. The code employs a 0-D approach for all components except the turbine, for which a one-dimensional design feature allows detailed assessment of cooling flows and expansion. The cooling model considers film cooling, thermal coatings, and multi-passage internal channels, ensuring accurate representation of advanced gas turbine performance.

3.1.1 Design and off-design simulations

Understanding GS in the context of this work involves distinguishing between design and off-design simulations. Design point performance is fundamental for engine concept design, optimization, and improvements. Off-design point performance examines steady-state variations under altered operational conditions, ensuring compatibility in mass flow, work, and rotational speed balances across components. Design point performance precedes other operational condition analyses.

Off-design component performance, specified through maps, poses challenges for GS, lacking support for loading maps and calculations for constraint convergence. Despite this limitation, an off-design in-flight simulation is crucial for aviation applications. A simplified off-design model in GS was developed and then verified using GasTurb [4], selecting cruising conditions for analysis due to data availability and operational relevance.

3.1.2 Verification of Thermodynamic Properties Calculations

GS relies on correlations from NASA Polynomials [14] to compute the thermodynamic properties of gases, fitting ideal gas behavior. Their validity is ensured within a temperature range of 300 to 5000 K. Since our study extends beyond this range, a comparative analysis with REFPROP [12] was conducted for temperatures from 200 to 2000 K and pressures from 0.1 to 10 bar. At the conclusion of the study, actual ambient temperature and pressure data, provided by the International Standard Atmosphere (ISA) data for flight altitudes ranging from 0 to 12,500 meters, were employed to evaluate the actual errors within the context of aircraft flight condition. Specific heats of N_2, O_2, and Ar were calculated using both methods to ensure accuracy. Water vapor and CO_2, considered negligible, are excluded. Specific heat values serve as a good indicator that thermodynamic properties like enthalpy and entropy are calculated correctly.
In the most critical conditions, i.e., at $P = 10\,bar$ and $T = 200\,K$, deviations increase for all three species, reaching up to 3.5 - 6.2%. When considering the actual conditions under which the inflow exists, a significant reduction in deviations can be observed. In this case, the maximum values are less than 0.5%. This reduction is mainly attributed to the combination of decreasing temperature and pressure at higher altitudes, which mitigates the effects of real gases, rendering the ideal gas assumption more valid.
In conclusion, due to the limited impact of a more accurate calculation on the problem at hand, it was decided to proceed with the NASA Polynomials relations.

3.2. Modelling of Air Intakes and Nozzles in GS Software

GS lacks codes for dynamic intakes and nozzles simulation. The following sections address the need for incorporating these components and outline their modeling methods.
Given that turbofan engines typically exhibit subsonic flows at the inlet and, at most, transonic flows at the nozzle outlet, the model described is designed for these conditions.
Both processes are nearly adiabatic, with minimal heat transfer, and the absence of moving parts supports the assumption that stagnation temperature remains constant between the inlet and exit in both scenarios.

3.2.1 Air Intake

The effective operation of an aircraft engine hinges on the air intake system's design and functionality. For jet engines, maintaining low Mach number airflow (0.55 to 0.65) at the fan inlet is crucial. Deviations in the velocity profile can disrupt aerodynamics, potentially leading to blade failure. The inlet behaves like a diffuser.
The intake must adapt to varying incident stream conditions based on flight speed and mass flow requirement (Fig. 1). Streamline behavior affects stagnation pressure losses, dependent on engine aspirated volumetric flow rate and flight Mach number, as shown in Fig. 5. The stagnation pressure ratio π_d is a function of corrected engine airflow and flight Mach number. Corrected air flow accounts for density variation with altitude.

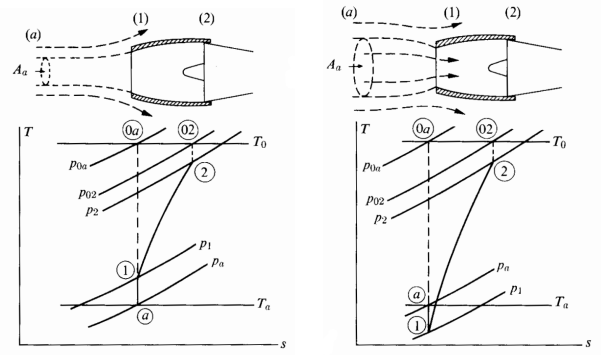

(a) *High speed or low mass flow* (b) *Low speed or high mass flow*

Figure 1: Typical streamline patterns for subsonic inlets [10]

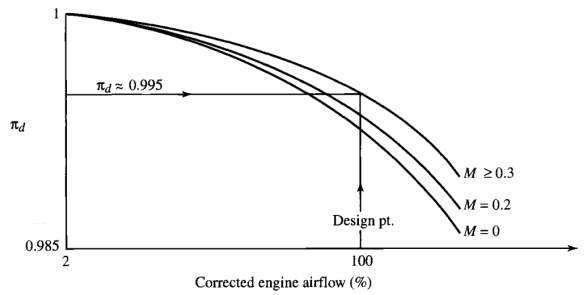

Figure 2: Typical subsonic inlet total pressure ratio [13]

Known fluid conditions are those infinitely upstream, i.e. undisturbed ambient air at the flight altitude. Stagnation pressure ratio is estimated through linear interpolation for flight Mach numbers from 0 to 0.2 and frmo 0.2 to 0.3. An iterative cycle for determining exit velocity at a known Mach number is needed considering the dependence of speed of sound on static temperature. This scheme is also applied when determining exit velocities for hot and cold flows from the LP turbine and fan, respectively.

3.2.2 Nozzle

The propulsive nozzle converts thermal energy to kinetic energy, generating thrust through high-speed fluid expulsion. This transformation occurs through an expansion process, controlled by pressure.
Predicting nozzle thermodynamic performance involves describing two main loss sources:

- **Fluid Dynamic Losses within the duct:** These arise from friction and possible boundary layer separation. Coefficients are commonly employed to estimate real flow conditions at the outlet starting from isentropic expansion. Although details of geometric variables impact losses, adopting an isoentropic efficiency η_n as defined in Eq. (1) has been considered a suitable compromise between modeling simplicity and result reliability.

$$\eta_n = \frac{h_{T,in} - h_{out}}{h_{T,in} - h_{out,is}} \tag{1}$$

- **Losses Downstream of the Exit Section:** If the expansion ratio remains below the critical ratio, the flow is entirely subsonic. In under-expanded cases, supersonic post-expansion leads to jet widening, causing significant losses due to interactions with the external environment. However, for net thrust propulsion evaluation, introducing additional parameters to model these losses downstream of the nozzle exit section is unnecessary.

The presence of two distinct flows leads to separate exhaust turbofans and mixed-stream turbofans as configurations. Mixed-stream turbofans can offer a 2–3% improvement in specific thrust and thrust-specific fuel consumption compared to separate exhaust turbofans [9] [15].
Further exploration is needed to understand operational parameter changes between the two designs. A study with a fixed bypass ratio (BPR) and variable fan compression ratio (β_{fan}) helps comprehend differences. The mixing of flows introduces a β_{fan} constraint, requiring equal static pressures at the mixer inlet. In separate flows, β_{fan} can be chosen freely, but an optimal value exists. An honest comparison between optimal separate flow and mixed-stream solutions reveals no substantial performance differences, but low-pressure spool components differ significantly. For mixed engines, the optimized β_{fan} is significantly lower, offering an opportunity to compensate for mixer weight with fewer LP turbine stages.
A simplified model has been employed to account for losses in the mixing process and a non-uniform temperature distribution at the end of the mixing chamber. A mixing efficiency has been directly integrated into the momentum balance equation. With higher BPRs, it becomes increasingly difficult to achieve a uniform temperature distribution, so mixing efficiency drops. This, coupled with the decreasing outperformance as BPR increases, leads to the conclusion that mixed flow turbofans offer better thermal efficiency and SFC only for modest BPRs.
To determine the downstream flow conditions of the mixing chamber, solving mass balance, momentum balance, and energy balance is needed. Two different approaches for modeling the mixing chamber have been described:

1. constant exit section equal to the sum of the inlet areas of the two flows;
2. isobaric mixer, which implies a variable-geometry exit section that depends on the operating conditions

The resulting system consists of 4 equations implicit in 4 unknowns. The Newton-Raphson iterative method, based on finite difference derivative calculations, has been employed to solve the problem.

4. Case study

To validate the model, referencing experimental data from a representative engine is ideal. Typically conducted on a test bench or on-wing, these measurements provide reliable information for various thermodynamic points. Unfortunately, proprietary data and actual component maps are not publicly available. Still, other publicly accessible sources offer a comprehensive overview of the analyzed reference engine.

4.1. Reference engine: General Electric CF6-80C2

The study adopts the GE CF6-80C2 as the reference engine for model validation—a dual-rotor, turbofan engine with a high BPR, variable stator geometry, and unmixed exhaust. The engine configuration comprises a single-stage fan and a 4-stage booster balanced by a 5-stage low pressure turbine (LPT) and a 14-stage high pressure compressor HPC balanced by a two-stage high pressure turbine (HPT). The GE CF6-80C2 is a high BPR turbofan designed for subsonic commercial airline service. It provides about 80% of thrust via the fan. The choice of this engine stems from the research group's expertise at Politecnico di Milano, ensuring reliability in interpreting results.

4.2. Design point simulation: takeoff conditions

This section details the modeling procedure for the thermodynamic system, laying out key assumptions critical for interpreting results. Potential energy variation, secondary systems like HPT and LPT clearance control, lubrication, ignition, and fuel injection are neglected. These exclusions are not expected to significantly impact performance estimation.
The plant layout is implemented in GS software format, assigning identifiers to components. Fig. 3 illustrates the process flow.
Two coolant flows are indicated: the first from the HPC discharge and the second upstream of the HPC. The first flow is for cooling the first stator, where high pressures are needed to inject the coolant. The second flow is for cooling subsequent rows, where lower pressure is required to circulate the coolant.
Exhaust Gas Temperature (EGT) is actively monitored in gas turbines, measured between the HPT and LPT for dual-rotor engines like CF6-80C2. Maintaining EGT margin ensures safety and longevity. A margin of 50-100°C is considered a safe operating practice to prevent stress, promote longevity, and avoid frequent overhauls and maintenance.
Selected β_{fan} aligns with literature for subsonic turbofans with comparable BPR. Compression ratio distribution between bypass and core flows is assumed to be the same, neglecting the stratification in high BPR fans. While this underestimates compression ratios for subsequent stages, OPR remains constant, leading to minor changes in overall performance.
Component polytropic efficiencies are adopted, offering a basis for comparing compressors/turbines with different compression/expansion ratios. Remaining values are derived from literature and adapted parameters from the stationary LM6000 gas turbine, reviewed and discussed by researchers at Politecnico di Milano.
The constraints necessary for proper system functioning are incorporated in the GS software input file's final section. Variables are categorized into independent and dependent, allowing users to specify convergence types and variable reassignment methods. Key conditions include mechanical power balance at HP and LP shafts and providing a suitable EGT margin, which is computationally intensive. The geometry of the two turbines and the fuel flow rate will adjust accordingly.

4.3. Off design point: cruise conditions

Cruise conditions denote the phase where an aircraft maintains a constant speed and altitude over an extended period. Unlike takeoff, maximum engine performance isn't crucial during cruise. However, these conditions significantly influence design, particularly for components like turbomachinery. In civil aviation, optimizing overall efficiency during most flight time reduces operational costs tied to fuel con-

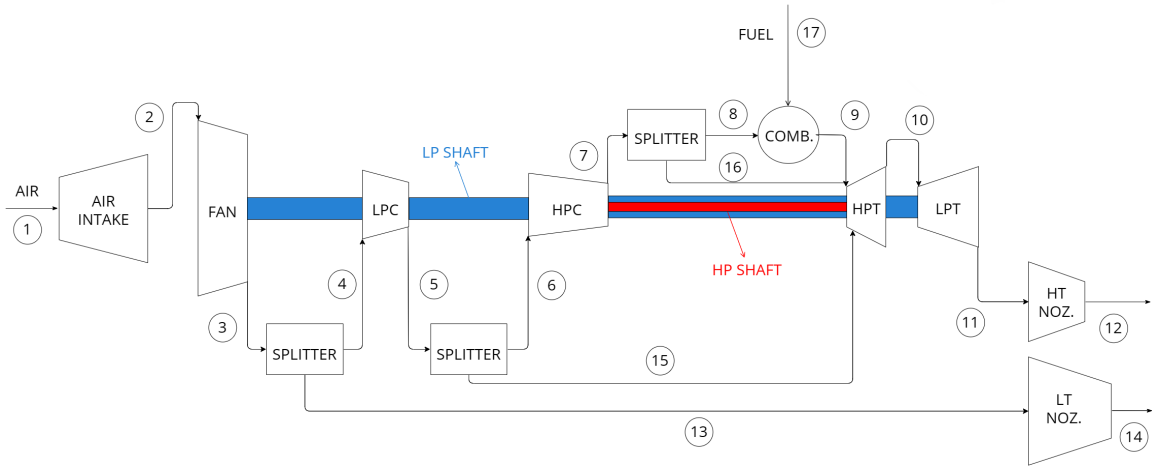

Figure 3: Process flow diagram

sumption. Hence, cruise conditions were chosen as an additional validation point for the model.

4.3.1 Aircraft drag estimation

In-flight, an aircraft contends with two primary aerodynamic forces: lift and drag. Using drag polar curves is a good approach for aircraft performance in simplified models. This curves illustrate drag-lift coefficient relationships, eliminating angle of attack dependency. For wings with Aspect Ratio AR > 3 and without extensive low drag buckets, a parabolic drag polar equation

$$C_D = C_{D0} + kC_L^2 \tag{2}$$

proves accurate within certain lift coefficient values. C_{D0} represents the zero-lift drag coefficient, accounting for the aircraft's overall parasitic drag, while wingtip vortices and non-uniform pressure around wings are accounted with the lift-induced drag coefficient k. Boeing 747-400 was chosen for this study because it is equipped with 4 CF6-80C2 engines.
The lift coefficient can be determined by balancing the weight of the aircraft. For this specific aircraft and other models C_{D0} and k were determined by Hoekstra et al. [16] using a stochastic total energy model. The results were then validated through CFD simulations. Additional considerations include wave drag at high Mach numbers, modeled by evaluating drag divergence Mach number and critical Mach number. Beyond the latter, the formation of shock waves, particularly on wing and turbomachinery surfaces, increases drag nonlinearly. A corrected zero-lift drag coefficient incorporates wave drag effects.

4.3.2 Off-design behavior of the system

Turbomachinery, heat exchangers, and other components are sized for average operating conditions, adapting to changes in boundary conditions.
Describing turbomachinery behavior is one of the main task to solve in off-design analysis. For compressible fluids, dimensionless reduced flow rate and speed are used, alongside compression/expansion ratio and isentropic efficiency. Air mass flow rate changes with altitude due to density variation. HP and LP shaft speeds are known, but compression and expansion ratios are derived from geometrical and thermo-fluid dynamic considerations. Constraints include adjusting peripheral speeds to maintain turbine geometry, balancing HP and LP shafts, keeping HPT cooling circuit areas constant, maintaining radiative thermal losses, and accounting for turbine choked flow conditions. In the absence of component maps, user-defined compressor efficiencies in GS have to increase slightly moving from takeoff to cruise conditions. The efficiency of the HPC, having 5 VGVs, will vary less. On the other hand, it is possible to consider the efficiency of the two turbines constant for the choked flow condition. The results of the analysis conducted with GasTurb software and discussions with highly qualified professionals in the university environment [5] enhance reliability in values used.

4.4. Implementation of the hydrogen system

After validating new components, hydrogen replaced conventional jet fuel, prompting exploration of novel plant schemes involving high-pressure turbine cooling using cryogenic hydrogen. Colder flows for turbine blade cooling offer positive effects by reducing the fraction of air processed by the compressor that doesn't enter the combustion chamber, while minimizing fluid-dynamic irreversibilities during the blade film-cooling process.
The plant layout was modified again to assess an additional cooling process: compressor air intercooling. Compressor work is expected to decrease when an intercooler is placed before.
Released heat is recuperated pre-heating the fuel, lowering the heat required in the combustion process. Regenerative fuel heating becomes crucial for LH2 due to its impact on cycle efficiency when introducing low-temperature fuel into the combustor.
Thrust-specific fuel consumption (TSFC) may not be suitable for comparing engines with different energy densities. Instead, thrust-specific energy consumption (TSEC) is more appropriate. TSEC is defined as the product of TSFC and the lower heating value (LHV) of the fuel.

4.4.1 Preliminary considerations

To mitigate inaccuracies arising from extremely low hydrogen temperatures (T $<$ 200 K), REFPROP [12] was utilized to calculate specific enthalpy values, then manually inserted into the GS software. Hydrogen exists in two isomeric forms: ortho-hydrogen and para-hydrogen. At room temperature, hydrogen is predominantly normal hydrogen, consisting of approximately 75% ortho-hydrogen and 25% para-hydrogen. However, below 180 K, a shift toward predominantly para-hydrogen occurs. This transition affects thermodynamic property calculations, leading to deviations in specific heat of up to 20-30%. The actual composition depends on internal reaction kinetics, but for calculations, an equilibrium condition was assumed, integrating REFPROP's normal hydrogen with an equilibrium dataset from studies by Le Roy et al. [11].

4.4.2 Modification of the thermodynamic cycle

Two additional heat exchangers, "HX 1" and "HX 2," were incorporated into the modified plant layout shown in Fig. 4, introducing a user-defined specific enthalpy drop for the hydrogen stream.
Under the assumption of nearly unchanged aircraft weight and shape, the hydrogen case without cooling was selected as the reference thrust value.
Compressor pressure ratios, ingested airflow, and BPR were held constant across all cycle investigations, while turbine inlet temperature (TIT) adjusts to meet thrust requirements. The

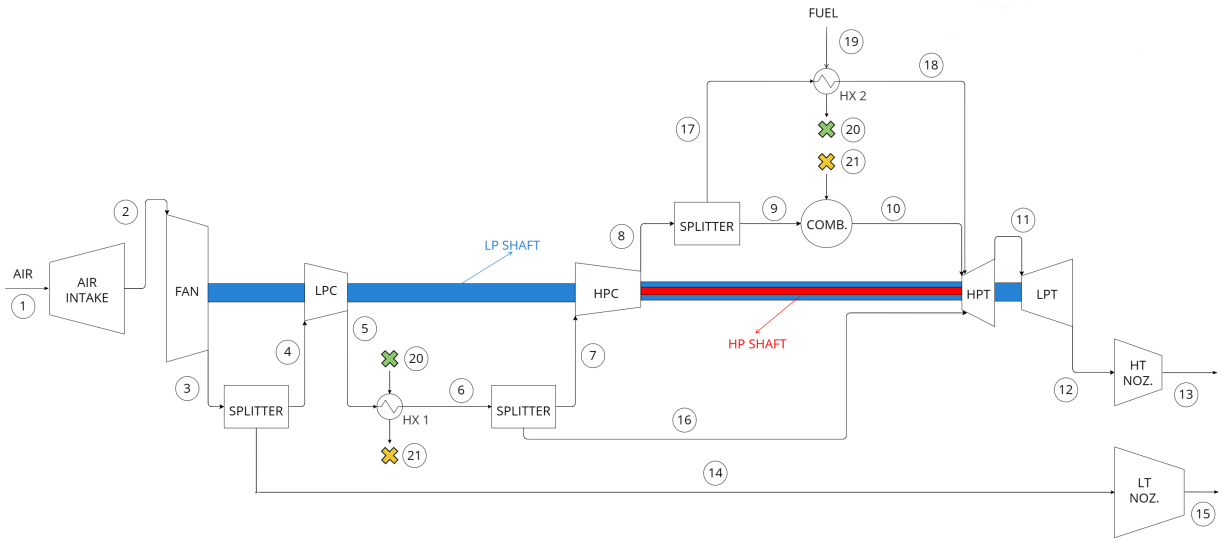

Figure 4: Process flow diagram - LH_2

configuration of turbine cooling-air was modified to enhance heat exchange, incorporating in Flow 17 the cooling of both the first stator and rotor of the HPT.
Strategically positioning a compressor intercooler in a turbofan setup is crucial for efficiency. It lowers compressor power consumption and reduces machine size by maintaining a higher fluid density. While placing it before the fan could benefit various components, technical-economic considerations, including added weight and potential freezing issues, favor a more conservative placement before the HPC. This choice balances thermodynamic advantages with practical engineering constraints.

5. Results & Discussion

5.1. Conventional cycle validation

The validation process involves thrust and thrust-specific fuel consumption (TSFC) comparisons with a reference engine (Table 1). Deviations are observed, especially in TSFC at takeoff. Although GS resulting thrust is higher, it suggests TSFC inaccuracies stem from fuel-related calculations. This highlights fuel mass flow rate estimation challenges due uncertainties related to lower heating values of jet fuel. Inaccurate sources for reference data could also play a role. Nevertheless, qualitative trends by varying flight Mach number (Fig. 5), together with TIT values, align closely with Mattingly's guidelines [13].
Deviations in cruise thrust and TSFC are quite small considering simplified off-design model and approximate drag estimation.
Despite complexities, the modular GS code remains adaptable for different jet engines and potential adjustments.

5.2. Hydrogen as fuel

The hydrogen-powered turbofan software results aim to assess improvements and identify potential issues from fuel replacement, focusing only on takeoff conditions. Analyzing a higher power settings may reveal more deviations and enhance understanding of fuel replacement implications.

Table 1: Results obtained versus expected results

	Takeoff			Cruise		
	Data	GS	Deviation	Data	GS	Deviation
Thrust [kN]	254.26	260.68	2.46%	54.01	53.55	-0.85%
TSFC [g/kN/s]	9.2	9.681	4.97%	15.98	15.42	-3.50%

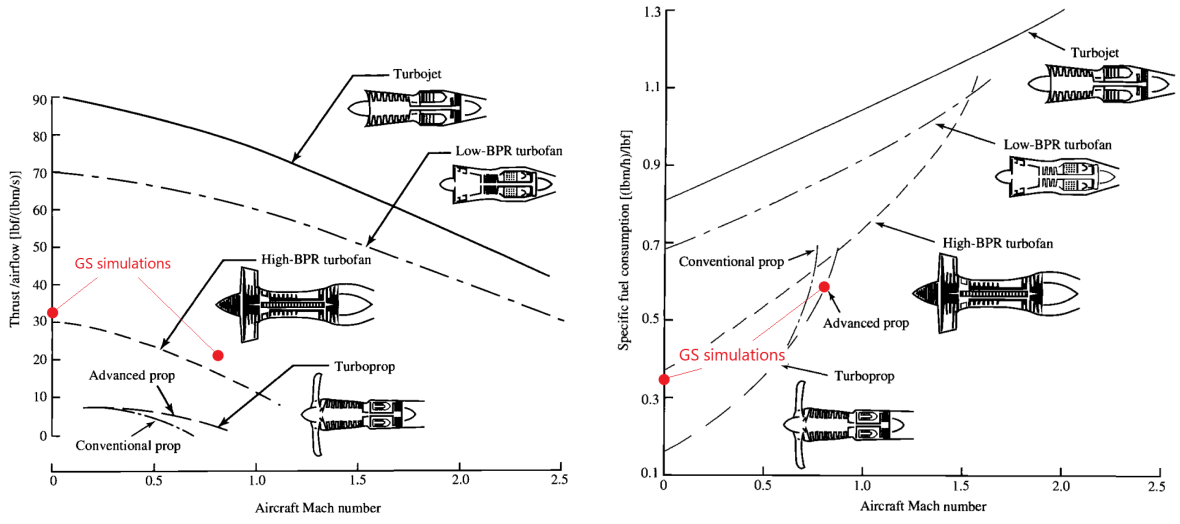

(a) *Specific thrust characteristics of typical aircraft engines*

(b) *Thrust-specific fuel consumption characteristics of typical aircraft engines*

Figure 5: Comparison with literature [13] - main figures of merit

5.2.1 Effects of fluid composition variation

The initial hydrogen analysis solely involves fuel substitution without alterations to the thermodynamic cycle, plant layout, or incoming flow temperatures/pressures.
Results reveal a 2.93% increase in propulsive thrust, primarily driven by a varied fluid composition in the turbine, leading to higher specific volume and lower expansion ratio. TSEC rises by 1.18%, attributed to increased energy needed for heat up hydrogen combustion products (mainly water vapor). However, to better explain the effects on fuel consumption, it is more correct to refer to a case with the same thrust. A second simulation varying TIT showed that a TIT reduction of 41°C allows to have the same thrust of 260.68 kN with a reduction of TSEC of 3.21%. Enthalpy drop in both HPT and LPT stages rises by around 1.5%, impacting turbine pressure ratios. Different combustion products reduce exhaust molar mass by 4.62%, affecting heat transfer coefficients and coolant flow in turbine blades. The exhaust mass flow decreases due to hydrogen's high calorific value, while HPT volumetric flow increases by 3.5%.

5.2.2 Evaluation of liquid hydrogen cooling capabilities

Fig. 6 evaluates the combined effects of two cooling methods and distinguishes their individual impacts. The analysis covers hydrogen-specific enthalpy drops from 0 to 4500 kJ/kg. Comparisons will be made referring to the hydrogen case without cooling ($\Delta h_{HX1} = 0\,kJ/kg$). Initially, turbine cooling air heats hydrogen in the HX 1 heat exchanger. Above 1750 kJ/kg, HX 2 is introduced, where hydrogen cools the core flow from the booster compressor.
Hydrogen temperature exhibits almost linear trends in Fig. 6a. The imperfect linearity is due to variations in specific heat. At supercritical conditions (P $\approx$ 50 bar), the heating process near critical conditions impacts specific heat.
Fig. 6b shows rapid HPT cooling air temperature drop in the range 0-1750 kJ/kg. When HX 2 starts to work as well, both inlet and outlet temperatures are affected. However, the outlet temperature decreases more than the inlet one because the coolant will have a lower flow rate. In fact, to keep the blade material below the limit temperature with a lower TIT, less coolant flow rate is required, especially if it is tapped at a lower HPC outlet temperature. This aspect highlights how reversing the order of the two exchangers along the hydrogen circuit could be beneficial because the use of an intercooler brings both classical advantages in compressor work and a reduction in HPT coolant flow rate. As thermodynamics improve, TIT gradually decreases (Fig. 6c), reducing H2 needed in the combustion chamber, driving TSEC reduction (Fig. 6d). The marked difference in TSEC trends between 0-1750 kJ/kg and 2000-4500 kJ/kg highlights the different effectiveness of the two cooling methods. While using HX 1 reduces TSEC by 0.34% for a $\Delta h_{HX1} = 1750\,kJ/kg$, the HX 2 intercooler provides an additional 1.84% reduction for a $\Delta h_{HX2} = 2750\,kJ/kg$.
Real application benefits are constrained by heat exchanger effectiveness and air side pressure drop.

6. Conclusions & Possible future developments

Our in-house software models nozzle and intake components, assessing jet engine thermodynamic performance at different altitudes and flight speeds. Integration with existing routines is successful, validated by replicating the GE CF6-80C2 engine operation. Discrepancies are minor, mainly due to reference data inaccuracies and highly simplifying assumptions. Expanding capabilities for supersonic flights could leverage hydrogen's cooling abilities and high flame speed.
Simply replacing jet fuel with hydrogen yields a 3% improvement in thrust-specific energy consumption, mainly driven by different turbine working fluid composition.
Utilizing liquid hydrogen cooling additionally reduces consumption by around 2%. Intercooler use proves 4.5 times more effective than cooling flows directly before the turbine. Considerations about pressure losses, heat exchanger efficiency, partially compensated by film cooling-related turbine losses, limit actual benefits in real applications. Having a lower temperature flow at the exit of the high-pressure compressor could unlock the development of cycles with higher

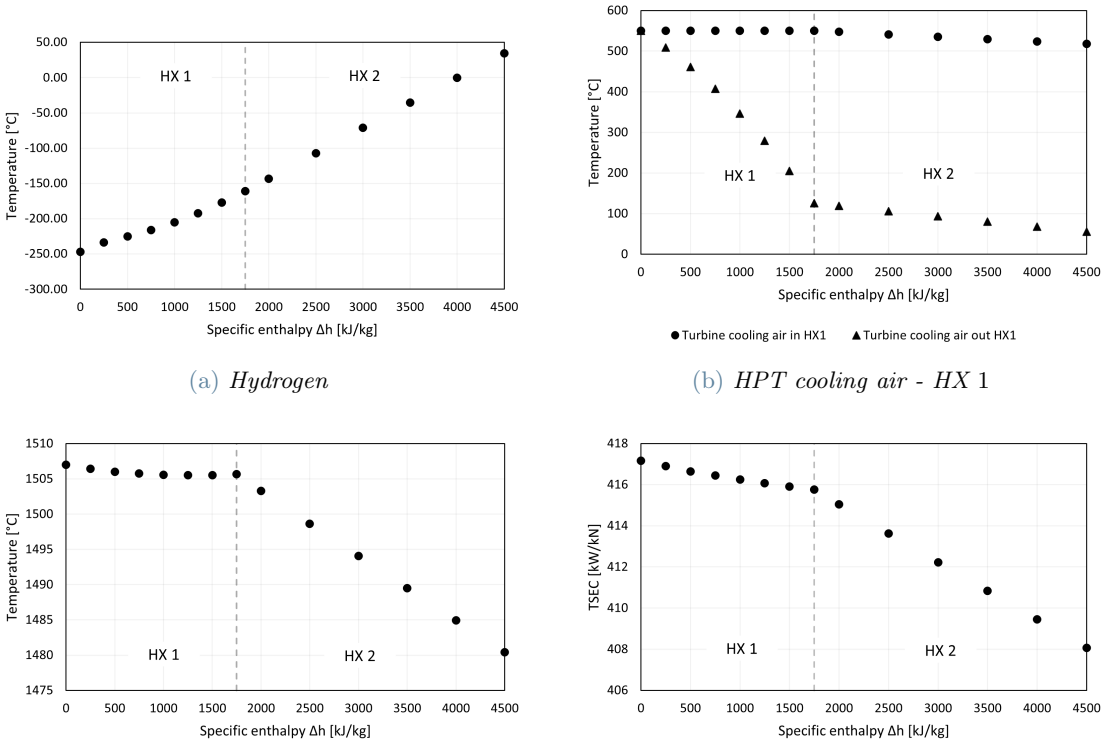

(a) *Hydrogen*

(b) *HPT cooling air - HX* 1

(c) *High pressure turbine inlet temperature*

(d) *Thrust specific energy consumption*

Figure 6: Specific enthalpy parametric study results

maximum temperatures and compression ratios for high specific thrust applications. There are many possible future developments, but they need to be supported by thorough technical and economic feasibility studies, especially for fuel storage, hydrogen production process and combustion.

References

[1] IEA (2023), Tracking Clean Energy Progress 2023, IEA, Paris https://www.iea.org/reports/tracking-clean-energy-progress-2023, License: CC BY 4.0.

[2] Airbus, Airbus reveals new zero-emission concept aircraft, 2020.

[3] Pratt & Whitney, Pratt & Whitney awarded department of energy project to develop hydrogen propulsion technology, 2022.

[4] GasTurb 14 user manual | GasTurb Gmbh | RWTH Aachen University, Aachen 52062.

[5] Chiesa, Paolo. Full professor full time at Politecnico di Milano - Energy department | Verbal discussion with thesis supervisor. November 2023.

[6] Eytan J. Adler and Joaquim R.R.A. Martins. Hydrogen-powered aircraft: Fundamental concepts, key technologies, and environmental impacts. *Progress in Aerospace Sciences*, 141:100922, 2023. Special Issue on Green Aviation.

[7] G D Brewer, R E Morris, G W Davis, E F Versaw, and G R Cunnington, Jr. Study of fuel systems for lh2-fueled subsonic transport aircraftvolume 2. final report, september 1976–december 1977. 7 1978.

[8] Paolo Chiesa and Ennio Macchi. A thermodynamic analysis of different options to break 60 *Journal of Engineering for Gas Turbines and Power-transactions of The Asme - J ENG GAS TURB POWER-T ASME*, 126, 10 2004.

[9] T. H. Frost. Practical bypass mixing systems for fan jet aero engines. *Aeronautical Quarterly*, 17(2):141–160, 1966.

[10] P.G. Hill and C.R. Peterson. *Mechanics and Thermodynamics of Propulsion*. Addison-Wesley, 2009.

[11] Robert J. Le Roy, Steven G. Chapman, and Frederick R. W. McCourt. Accurate thermodynamic properties of the six isotopomers of diatomic hydrogen. *The Journal of Physical Chemistry*, 94(2):923–929, 1990.

[12] E. W. Lemmon, I. H. Bell, M. L. Huber, and M. O. McLinden. NIST Standard Reference Database 23: Reference Fluid Thermodynamic and Transport Properties-REFPROP, Version 10.0, National Institute of Standards and Technology, 2018.

[13] J.D. Mattingly, K.M. Boyer, and H. von Ohain. *Elements of Propulsion: Gas Turbines and Rockets*. AIAA education series. American Institute of Aeronautics and Astronautics, Incorporated, 2016.

[14] Bonnie McBride, Michael Zehe, and Sanford Gordon. Nasa glenn coefficients for calculating thermodynamic properties of individual species. 10 2002.

[15] H. Pearson. Mixing of exhaust and by-pass flow in a by-pass engine. *The Aeronautical Journal*, 66(620):528–530, 1962.

[16] Junzi Sun, Jacco Hoekstra, and Joost Ellerbroek. Aircraft drag polar estimation based on a stochastic hierarchical model. 2018.

[17] A Westenberger. Liquid hydrogen fuelled aircraft—system analysis, cryoplane. *European Commission, Final Report No. GRD1-1999-10014. https://cordis. europa. eu/project/id/G4RD-CT-2000-00192*, 2003.